

# Exploring the Role of Vacuum Fluctuations on Nuclear-Lepton Interactions in Atomic Systems

Aliyu Adamu\*

Department of Physics, University of Maiduguri, Maiduguri, Nigeria.

Received: 1 Sep. 2023, Revised: 22 Nov. 2023, Accepted: 29 Nov. 2023.

Published online: 1 Jan 2024.

**Abstract:** Fruit peel extracts of irradiated *Punica granatum* were inspected under laboratory conditions for their insecticidal activities against the Rice weevil, *Sitophilus oryzae* adults and compared with the extract obtained from unirradiated peels. Both the unirradiated and the irradiated extract caused different mortality, where the irradiated extract was the highest effect. Obtained results revealed that the highest mortality of unirradiated extract at concentration of 8% was 36.7% after 96 hours while irradiated extract with 10 KGy showed highly mortality 93.3% at same concentration and time. The data indicated that unirradiated extract had attractive effect. The results showed the opposite results when filter paper treated with irradiated pomegranate extract, the repellent effect increased with increasing the extract concentration. The highest effect was demonstrated after 2 hours, which the repellency percentage reached 93.3%. The effect of 10KGy of gamma radiation on total phenolic content and antioxidant activity of pomegranate peel powder was studied. Comparing irradiated pomegranate peel powder to unirradiated peel, a substantial rise in the percentage of total phenolic content and antioxidant activity were observed. Also, the components of the ethanolic extract from unirradiated and irradiated pomegranate peel were identified by HPLC analysis.

**Keywords:** *Sitophilus oryzae*, Gamma radiation, Pomegranate peels extract, Repellent, Toxicity, Total phenolic content, antioxidant activity, HPLC.

## 1 Background

The interaction between a lepton and a nucleus in an atomic system is typically described by the point-charge  $Z/r$  nuclear potential, which assumes the lepton and nucleus are point-like particles [1]. However, this model fails to take into account the finite-size charge distribution of both particles, which arises due to their interaction with external fields, such as the fluctuating vacuum fields. To incorporate these effects, the  $Z/r$  potential must be modified, resulting in a perturbation on the Hamiltonian that describes the system [2-4]. To solve for this modified Hamiltonian, various approximation methods have been employed, with time-independent perturbation theory being the most commonly used [5-8]. The first-order perturbation theory is crucial in atomic and nuclear physics, as it allows for the calculation of small changes in lepton energy states due to various effects, including relativistic and spin-orbit effects, nuclear finite-size effects, and effects due to vacuum polarization and fluctuations in the vacuum fields [9-18]. These corrections to the energy levels have paved the way for more precise measurements of fundamental

physical constants and the determination of nuclear radii [19-25].

In recent years, there has been increasing interest in the effects of vacuum fields on lepton-nuclear interactions [26,27]. These fields can affect the charge distribution and energy states of orbiting leptons, leading to further corrections to the energy levels and nuclear-lepton interaction models [28-32]. The finite-size nuclear models have provided valuable information about the nucleus, such as radii and quadrupole moments, but the effects of extended charged orbiting leptons and vacuum fields on the wavefunctions and quantum states of both the nucleus and its bound leptons remain unclear. This paper aims to determine the possible wavefunctions for two interacting finite-sized particles affected by vacuum fields and calculate the resulting changes in the quantum states of the leptons using the theoretical model developed in this study. This model provides a simplified description of the combined nuclear-lepton wavefunctions in terms of their separation distance and can help to further our understanding of lepton-nuclear interactions in atomic systems.

## 2 Methodology

The interaction of relativistic lepton with extended charge nucleus is affected by fluctuating electromagnetic fields in quantum vacuum. These

\* Corresponding author e-mail:

fields perturbed the lepton-nuclear interaction by an amount  $\vec{\varepsilon}$  as illustrated in Figure 1. The effective nuclear-lepton interaction can be obtained by adding

$$U_{eff}(\vec{r}, \vec{\varepsilon}) = \frac{1}{V} \left[ \int U(\vec{r}) d^3\varepsilon + \int \vec{\varepsilon} \cdot \nabla U d^3\varepsilon + \frac{1}{2} \int \varepsilon_i \varepsilon_j \frac{\partial}{\partial x_i} \frac{\partial}{\partial x_j} U d^3\varepsilon \right] \quad (1)$$

where for spherical symmetry the integrals,

$$\int U(\vec{r}) d^3\varepsilon = U(\vec{r}) \times V$$

$$\int \vec{\varepsilon} \cdot \nabla U d^3\varepsilon = \nabla U \cdot \int \vec{\varepsilon} d^3\varepsilon = 0$$

and

$$\begin{aligned} \int \varepsilon_i \varepsilon_j \frac{\partial}{\partial x_i} \frac{\partial}{\partial x_j} U d^3\varepsilon &= \lambda^2 \delta_{ij} \int \frac{\partial}{\partial x_i} \frac{\partial}{\partial x_j} U d^3\varepsilon \\ &= \frac{1}{3} \lambda^2 \nabla^2 U \delta_{ij} \end{aligned}$$

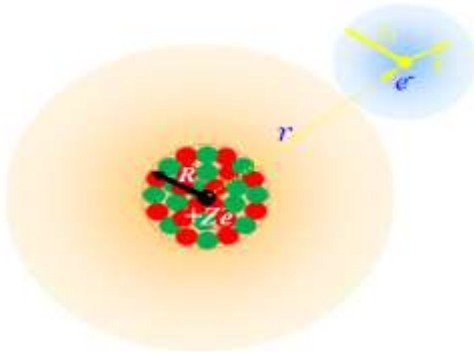


**Fig.1:** The sketch of nuclear-lepton charge distribution when interacts with fluctuation fields.

Therefore, equation 1 becomes,

$$U_{eff}(R, r_l) = U(R) + \zeta'(r_l) \quad (2)$$

where

$$\zeta'(r_l) = \frac{1}{6} \lambda_l^2 \nabla^2 U(R) \delta_{ij} \quad (3)$$

and the potential for extended charge nucleus is given by

$$U(R) = -\frac{Z\gamma}{2R} \left[ 3 - \left( \frac{r}{R} \right)^2 \right] \quad (4)$$

with radius  $R = r_0 A^{1/3}$ ,  $A$  the nucleon number,  $\lambda$  the Compton wavelength and  $\gamma = ke^2$ .

small perturbation  $\vec{\varepsilon}$  to the lepton position,  $U_{eff} = U(\vec{r} + \vec{\varepsilon})$  and can be expanded using Taylor's series as

Thus, the effective interaction (1) can be simplified to give

$$U_{eff}(R, \lambda_l) = -\frac{Z\gamma}{2R} \left[ 3 - \frac{1}{A^{1/3}} \left( \frac{r}{r_0} \right)^2 - \frac{1}{3A^{1/3}} \left( \frac{\lambda_l}{r_0} \right)^2 \right] \quad (5)$$

The solution to the effective interaction (5) can be sought from time independent perturbation theory,

$$\begin{aligned} \hat{E}'_n(\lambda) &= \langle \psi_n | \hat{H}_0 | \psi_n \rangle + \lambda \langle \psi_n | \hat{H}_{pert.} | \psi_n \rangle \\ &+ \lambda^2 \sum_{m \neq n} \frac{|\langle \psi_n | \hat{H}_{pert.} | \psi_m \rangle|^2}{\hat{E}_n - \hat{E}_m} + \mathcal{O}(\lambda^3) \end{aligned}$$

where  $\hat{E}'_n$  is the 0<sup>th</sup> order correction to the  $n^{\text{th}}$  eigenvalue, and  $\psi_n$  is the 0<sup>th</sup> order correction to the  $n^{\text{th}}$  eigenfunctions;  $\hat{E}_n^{(1)}$  is the first order corrections;  $\hat{E}_n^{(2)}$  is the second order corrections  $\lambda$  is taken to be dimensionless small number,  $\lambda \ll 1$  and  $\mathcal{O}(\lambda^3)$  is the Landau symbol [4,6,7,33]. The first-order correction to lepton energy states due to lepton extended wavefunctions is given by

$$\hat{E}_{nlm}^{(1)} = \int \psi_{nlm}^* U_{eff}(R, \lambda_l) \psi_{nlm} d\tau \quad (6)$$

where the  $\psi_{nlm}$  is the unperturbed wavefunction and its intensity corresponding to  $n00$  states is given by:

$$|\psi_{n00}|^2 = \begin{cases} \frac{z^3}{\pi n^3 a_0^3}; & l = 0, m = 0 \\ 0 & l \geq 1 \end{cases} \quad (7)$$

where  $a_0 = \hbar^2/kme^2$ , is the Bohr radius. The shift in  $n00$  energy states are determined using (6) as,

$$\begin{aligned} \Delta E_{n00}^{(1)} &= -\frac{Z\gamma}{2R} \int_0^R \left[ 3 - \left( \frac{r}{R} \right)^2 - \frac{1}{3} \left( \frac{\lambda_l}{R} \right)^2 \right] |\psi_{n00}|^2 r^2 dr \\ &= E_n \frac{z^2}{n} \left( \frac{16A^{1/3}}{5} \rho_l - \frac{4}{9} \sigma_l \right) \quad (8) \end{aligned}$$

where for an electron  $\rho_e = (r_0/a_0)^2 = 5.14577921 \times 10^{-11}$ ,  $\sigma_e = (\lambda_l/a_0)^2 = 7.09401373 \times 10^{-10}$  and  $\lambda_l = 1.4089698 \times 10^{-15} \text{ m}$  [34].

### 3 Results

The interaction (8) is analyzed using Microsoft Excel package and Figure 2(a), (b), (c), (a), (d), (e) and (f) gives the information on variation of the nuclear-nuclear wavefunction  $U(R, \lambda)$  with distance  $r$  from the origin of the single-lepton atoms: *Li*, *Na*, *K*, *Rb*, *Sc* and *Fr*.

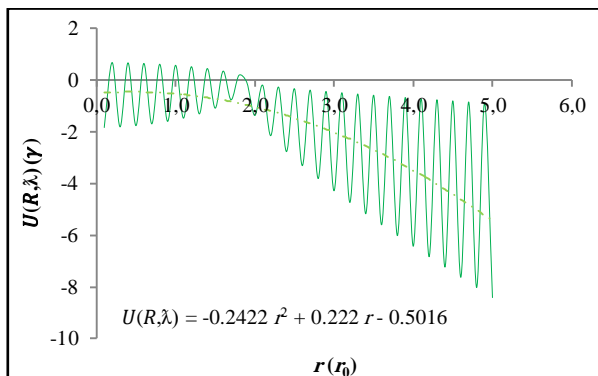


**Fig.2(a):** The lepton-nuclear wavefunctions for *Li* atom as a function of  $r$ .

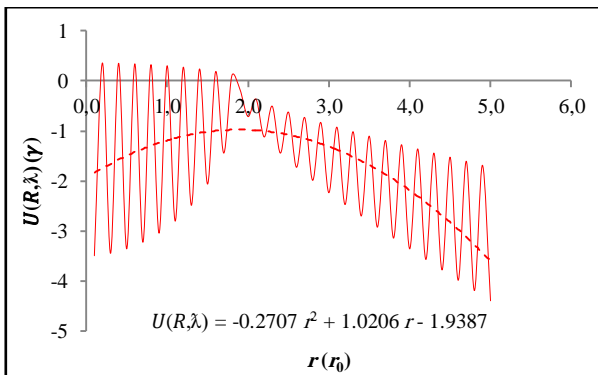


**Fig.2(b):** The lepton-nuclear wavefunctions for *Na* atom as a function of  $r$ .

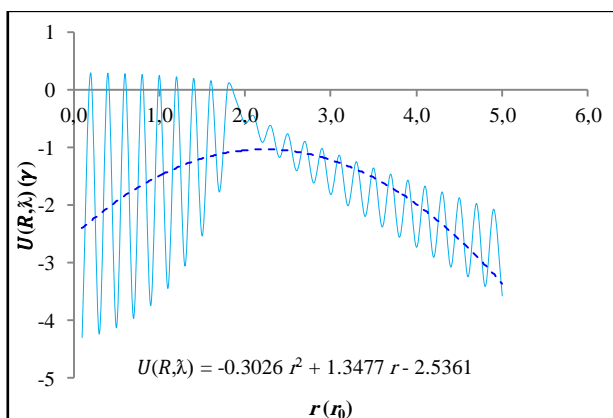


**Fig. 2(c):** The lepton-nuclear wavefunctions for *K* atom as a function of  $r$ .

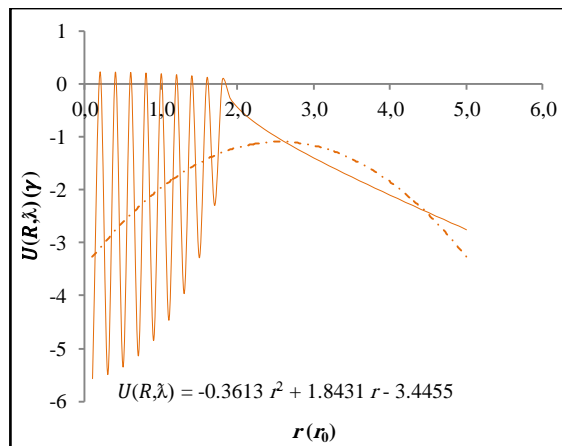


**Fig.2(d):** The lepton-nuclear wavefunctions for *Rb* atom as a function of  $r$ .

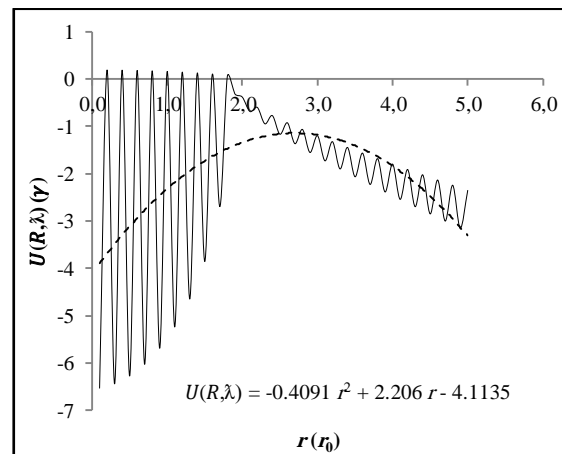


**Fig. 2(e):** The lepton-nuclear wavefunctions for *Sc* atom as a function of  $r$ .

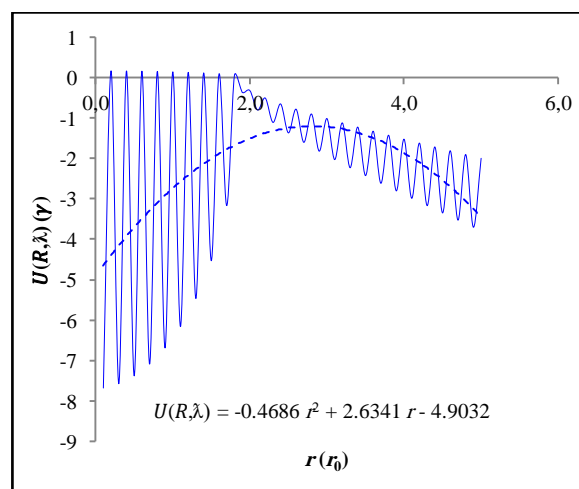


**Fig. 2(f):** The lepton-nuclear wavefunctions for *Fr* atom as a function of  $r$ .

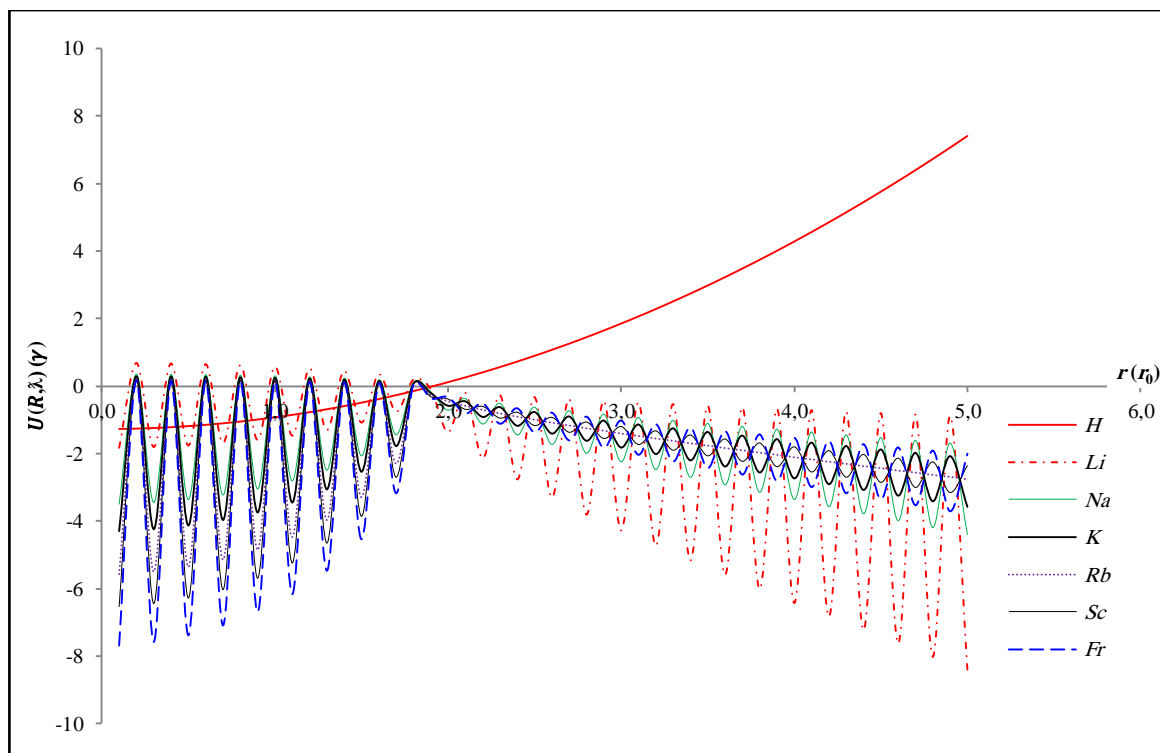


**Fig. 3:** The comparison of nuclear and lepton wavefunction as a function of distance  $r$  from the origin.

#### 4 Discussion

Figure 2 (a) to (f) showed a sinusoidal plot of  $U(R, \lambda)$  as a function of  $r$  visualizing the information of Equation 5 which was obtained from quantum electrodynamics' effects. The figures revealed different formation of wavefunction when extended charged lepton interacts with finite-size nucleus. There is an important characteristic of the potential at about  $r = 1.8 r_0$  exhibited by the entire nucleus (light, medium and heavy). This indicates the boundary between the nuclear and lepton wavefunctions. Figure 2 further interpreted the effective interaction (5) as having non-zero value at the origin ( $r \sim 0$ ), this contradicts the coulomb point-charge interaction which is infinite at origin. This indicates that the nuclear potential is concentrated towards the origin. This modified the coulomb interaction by giving the correct analytical behavior of the nuclear wavefunctions at origin. It can also be observed that the extension of the wavefunctions towards leptons have different characteristics as it starts increasing towards the origin of lepton charge.

Figure 2 were studied using the regression analysis and developed a simple relationship between  $U(R, \lambda)$  and the distance  $r$  that satisfied,

$$(R, \lambda) = -0.2422 r^2 + 0.2220 r - 0.5016$$

$$(R, \lambda) = -0.2707 r^2 + 1.0206 r - 1.9387$$

$$(R, \lambda) = -0.3026 r^2 + 1.3477 r - 2.5361$$

$$(R, \lambda) = -0.3613 r^2 + 1.8431 r - 3.4455$$

$$(R, \lambda) = -0.4091 r^2 + 2.2060 r - 4.1135$$

$$(R, \lambda) = -0.4686 r^2 + 2.6341 r - 4.9032$$

for *Li*, *Na*, *K*, *Rb*, *Sc* and *Fr* respectively. These equations show the potential-distance relationships that best suit the observed data from simulations. The  $r^2$  component emphasizes a quadratic dependence on distance, whereas the coefficients show the direction and strength of these dependencies. The potential's finite, non-zero value at  $r \approx 0$  suggests that the Coulomb interaction has changed, which gives nuclear wavefunctions at the origin a more realistic analytical behavior. The fitted functions reflect this change. The observed peak at  $r = 1.8 r_0$  in Figure 2 represents a transition or barrier between nuclear and lepton wavefunctions. The extension of nuclear wavefunctions towards leptons and the different properties detected as they approach the lepton's origin reveal the complex interplay between the charged lepton and the finite-size nucleus. The resulting equations are a valuable tool for understanding or predicting the behavior of the system beyond reported data points.

These results provide a quantitative explanation of the potential-distance connection within the context of quantum electrodynamics, and are important in understanding the behavior of wavefunctions and interactions between charged leptons and nuclei. The findings provide opportunities for further research, such as a closer look at the effects of the altered Coulomb interaction, a more thorough investigation of the physical meaning of the fitted coefficients, and the use of the model in different situations or systems.

Figure 3 gives the comparison of the variation of the effective interaction (5) with distance  $r$  from the origin of various atomic nuclei. The figure showed the finite behavior of the effective interaction at  $r = 0$ . For hydrogen atom, the wavefunction gives a curve stating form  $\gamma (= ke^2)$  to 0.8 at  $r = 0$  and then starts to increase with the increase in distance,  $r$  from the nucleus. The curve exhibited by hydrogen atom could be attributed to interaction between a proton and single lepton having roughly spherical charge distributions with no shielding effect. Other atomic nuclei have the wavefunctions decreasing to the origin of lepton charge distribution. This suggested that the effective interaction (5) is more effective at a point very close to the atomic nucleus and when there is no electron-electron interaction. Figure 3 also showed the dependence of lepton-nuclear interaction described by the theoretical model (5) as a function of the both lepton and nuclear position  $r$ . The nuclear wavefunction starting from  $r = 0$  to  $r \approx 1.8 r_0$ , describes the nuclear potential field and lepton wavefunction starts to exist at a distance  $r > 1.8 r_0$ , describes the lepton fields.

In this study, a new theoretical model of nuclear-electron interaction energy was formulated, which addresses the infinite value of  $Z/r$  potential at the origin ( $r \sim 0$ ) that results from the point-charge nuclear model. The proposed model provides a remedy for this problem and modifies the undefined nature of the  $Z/r$  potential. The findings from this study suggest that the effective interaction (5) has a non-zero value at the origin ( $r \sim 0$ ), unlike the coulomb point-charge interaction, which is infinite at the origin. This indicates that the nuclear potential is concentrated towards the origin, and it modifies the coulomb interaction by giving the correct analytical behavior of the nuclear wavefunctions at origin. The study also reveals different formations of wavefunction when an extended charged lepton interacts with a finite-size nucleus. The figures presented in this study show that there is an important characteristic of the potential at about  $r = 1.8 r_0$  exhibited by the entire nucleus (light, medium, and heavy), indicating the boundary between the nuclear and lepton wavefunctions. Moreover, the effective interaction (5) is more effective at a point very close to the atomic nucleus and when there is no electron-electron interaction. The proposed model

presents a theoretical framework for describing atomic systems and understanding the pattern in which both lepton and nuclear fields interact. It could play a vital role in the quantum mechanical description of atomic systems. Additionally, this lepton-nuclear effective interaction, which takes into account the finite size of both particles together with vacuum field effects, could reflect on the nuclear coulomb energy, atomic quantum states or be used in determining the possible wavefunctions for two interacting particles (leptons and nucleus).

## 5 Conclusions

In conclusion, the modified electron-nucleus interaction proposed in this study would provide a clear understanding of the physical structure and details of atomic spectra that will remarkably agree with the measured values. It would also affect the energy levels of an electron and thus needs to be involved in the general understanding of electron energy level corrections such as the fine structure, hyperfine structure, Lamb shift, and isotope shift.

## References

- [1] Greiner W and Maruhn JA. Nuclear Models. Springer-Verlag Berlin Heidelberg, Germany, 1996; pp 2, 218 – 219, 261.
- [2] Feranchuk I, Ivanov A, Le V-H, Ulyanenkov A. Non-perturbative Description of Quantum Systems. Lecture Notes in Physics 894, Springer International Publishing Switzerland 2015, XV, 362 pp 63 illus., 43 illus. in color, softcover. [https://doi.org/10.1007/978-3-319-13006-4\\_1](https://doi.org/10.1007/978-3-319-13006-4_1).
- [3] Landau LD and Lifshitz EM. Quantum Mechanics. Fizmatgiz, Moscow, 2004.
- [4] Greiner W. Quantum Mechanics: An Introduction. 4th Edition. Springer, Berlin, Germany, 2001, pp 181, 220 – 227.
- [5] Adamu A, Hassan M, Dikwa MK and Amshi SA. Determination of Nuclear Structure Effects on Atomic Spectra by Applying Rayleigh–Schrödinger Perturbation Theory, American Journal of Quantum Chemistry and Molecular Spectroscopy, 2018; 2 (2): 39-51.
- [6] Gasiorowicz S. Quantum Physics, Third Edition. John Wiley & Sons, Inc., the United States of America, 2003.
- [7] Das A and Sidharth B G. Revisiting the Lamb Shift. European Journal of Theoretical Physics. 2015; 12(IYL): 15-34
- [8] House JE. Fundamentals of Quantum Mechanics: 3rd Edition. Academic Press is an imprint of Elsevier, United Kingdom, 2018, pp 63.
- [9] Lee AR and Liesegang J. The Lamb shifts as a consequence of the Finite size of the Electron, Lettere Al Nuovo Cimento. 1972; 3(5): 29-33.



- [10] Patoary A-SM and Oreshkina NS. Finite Nuclear Size Effect to the Fine Structure of Heavy Muonic Atoms. *The European Physical Journal D*, 2018; 72: 54. <https://doi.org/10.1140/epjd/e2018-80545-9>.
- [11] DelPapa DF, Holt RA and Rosner SD. Hyperfine Structure and Isotope Shifts in Dy II, *Atoms*, 2017; 5: 5. <https://doi.org/10.3390/atoms5010005>.
- [12] Antognini A, Hagelstein F and Pascalutsa V. The Proton Structure in and out of Muonic Hydrogen. *arXiv:2205.10076v1 [nucl-th]* 20 May 2022. <https://doi.org/10.1146>.
- [13] Bethe HA. The Electromagnetic Shift of Energy Levels. *Physical Review*, 1947; 72: 339 – 341.
- [14] Carlson CE. The proton radius puzzle, *Prog. Part. Nucl. Phys.*, 2015; 82(59).
- [15] Dong J M, Zuo W, Zhang H F, Scheid W, Gu J Z and Wang Y Z. Correlation between Muonic Levels and Nuclear Structure in Muonic Atoms. *arXiv:1111.0494v1 [nucl-th]* 2 Nov 2011.
- [16] Elekina EN, Krutov AA, Martynenko AP. Fine Structure of The Muonic 4He Ion. *T. 8, No 4(167)*, 2011, page 554 – 563.
- [17] Faustov RN, Krutov AA, Martynenko AP, et al. 1S-2S Energy Shift in Muonic Hydrogen, *European Physical Journal, Web of Conferences*. 2019; 204. <https://doi.org/10.1051/epjconf/201920405005>. Baldin ISHEPP XXIV.
- [18] Godunov SI and Vysotsky MI. The Dependence of the Atomic Energy Levels on a Super Strong Magnetic Field with Account of a Finite Nucleus Radius and Mass, *arXiv:1304.7940v1 [hep-ph]* 30 Apr 2013.
- [19] Kanda S. A search for atomic parity violation in muonic atoms using a high-intensity pulsed muon beam at J-PARC. *European Physical Journal, Web of Conferences*. 2022; 262: 01010. <https://doi.org/10.1051/epjconf/202226201010>.
- [20] Kardaras IS and Kosmas OT. Using simulated annealing algorithms to solve the Schrödinger equation in muonic atoms. *Journal of Physics: Conference Series*. 2015; 574: 012168. <https://doi.org/10.1088/1742-6596/574/1/012168>.
- [21] Kena ED and Adera GB. Estimation of Relativistic Mass Correction for Electronic and Muonic Hydrogen Atoms with Potential from Finite Size Source. *Ethiopian Journal of Science and Sustainable Development*. 2022; 9(2): 68 – 77. <https://doi.org/10.20372/ejssdastu:v9.i2.2022.474>
- [22] Oreshkina NS. Self-energy correction to the energy levels of heavy muonic atoms. *arXiv:2206.01006v1 [physics.atom-ph]* 2 Jun 2022. <https://doi.org/10.48550/arXiv.2206.01006>.
- [23] Toth BC, Borsanyi Sz, Fodor Z, et al. Muon  $g - 2$ : BMW Calculation of the Hadronic Vacuum Polarization Contribution. *The 38th International Symposium on Lattice Field Theory*, LATTICE2021 26th-30th July, 2021, Zoom/Gather @ Massachusetts Institute of Technology, proceedings of science, PoS (LATTICE 2021) 005.
- [24] Welton Th. Some Observable Effects of the Quantum-Mechanical Fluctuations of the Electromagnetic Field. *Physical Review*. 1948; 74: 1157.
- [25] Maclay GJ. History and Some Aspects of the Lamb Shift. *Physics*. 2020; 2: 105–149. <https://doi.org/10.3390/physics2020008>.
- [26] Allehabi SO, Dzuba VA, and Flambaum VV. Theoretical study of electronic structure of hafnium (Hf,  $Z = 72$ ) and rutherfordium (Rf,  $Z = 104$ ) atoms and their ions: Energy levels and hyperfine structure constants. *arXiv:2109.13716v2 [physics.atom-ph]* 29 Sep 2021.
- [27] Carlson CE, Gorchtein M and Vanderhaeghen M. Nuclear Structure Contribution to the Lamb Shift in Muonic Deuterium. *arXiv:1311.6512v3 [nucl-th]* 27 Jan 2014.
- [28] Hsiang J-T and Hu BL. Atom-Field Interaction: From Vacuum Fluctuations to Quantum Radiation and Quantum Dissipation or Radiation Reaction. *Physics* 2019; 1: 430 – 444; <https://doi.org/10.3390/physics1030031>.
- [29] Naito T, Roca-Maza X, Colò G and Liang H. Effects of finite nucleon size, vacuum polarization, and electromagnetic spin-orbit interaction on nuclear binding energies and radii in spherical nuclei. *Physical Review C*, 2020; 101: 064311. <https://doi.org/10.1103/PhysRevC.101.064311>.
- [30] Rhys D. Perturbation theory in atomic physics, May 13, 2010.
- [31] Deck RT, Amar JG and Fralick G. Nuclear size corrections to the energy levels of single-electron and -muon atoms. *J. Phys. B: At. Mol. Opt. Phys*. 2005; 38: 2173–2186.
- [32] Niri BN and Anjami A. Nuclear Size Corrections to the Energy Levels of Single-Electron Atoms, *Nuclear Science*. 2018; 3(1): 1 – 8.
- [33] House JE. *Fundamentals of Quantum Mechanics: 3rd Edition*. Academic Press is an imprint of Elsevier, United Kingdom, 2018, pp 63.
- [34] Mei SY and Mei ZH. Theoretical Calculation and Proof of Electron and Proton Radius. *Journal of Physics and Astrophysics*. 2019; 7(3): 181.